Shape-based Human Detection for Threat Assessment

Dah-Jye Lee[a], Pengcheng Zhan[a], Aaron Thomas[a], and Robert Schoenberger[b]
[a] Department of Electrical and Computer Engineering, Brigham Young University, 459 CB, Provo, Utah 84602
[b] Agris-Schoen Vision Systems, Inc., 3320 Mill Springs Drive, Fairfax, VA 22031

ABSTRACT

Detection of intrusions for early threat assessment requires the capability of distinguishing whether the intrusion is a human, an animal, or other objects. Most low-cost security systems use simple electronic motion detection sensors to monitor motion or the location of objects within the perimeter. Although cost effective, these systems suffer from high rates of false alarm, especially when monitoring open environments. Any moving objects including animals can falsely trigger the security system. Other security systems that utilize video equipment require human interpretation of the scene in order to make real-time threat assessment. Shape-based human detection technique has been developed for accurate early threat assessments for open and remote environment. Potential threats are isolated from the static background scene using differential motion analysis and contours of the intruding objects are extracted for shape analysis. Contour points are simplified by removing redundant points connecting short and straight line segments and preserving only those with shape significance. Contours are represented in tangent space for comparison with shapes stored in database. Power cepstrum technique has been developed to search for the best matched contour in database and to distinguish a human from other objects from different viewing angles and distances.

Keywords:
Threat assessment, human detection, intrusion detection, shape analysis, machine vision, power cepstrum, tangent space

1. INTRODUCTION

An automated visual surveillance system is an intelligent system based on computer vision technology and built for the security purpose to detect and track human intrusion and vandalism. Computer vision techniques are used in such systems and human detection is one of the most important tasks. Much work has been done to achieve better human intrusion detection or even track their activities and movements. A good survey was done to review the techniques for human motion analysis [1-2], which deals with detecting, tracking and recognizing people. Some human intrusion detection systems detect human intrusion by locating and tracking human faces [3-5]. A method of reliably extracting face information based on an eigen mask was proposed [3]. A 3D module-based system was used to locate human faces under various conditions, i.e., facial-hair, occlusion and so on [4]. A new classification method using forest-structured Bayesian networks was used to discriminate face from non-face patterns [5].

Many human detection systems have been introduced in literatures. A computationally less intensive system which can detect and track up to two persons' activity was developed [6]. Information from multiple cameras was used and Neural Network algorithm deals with the activity classification, but empirical values are relied on heavily to help fasten the detection. A visual surveillance system based on simple shape parameters of silhouette patterns was discussed [7]. A good way of extracting the silhouette was addressed in the paper by resorting to some kind of brightness level transformation. It solved the occlusion problem which occurs when multiple people walk together passing the system. However, the whole algorithm is closely related to the selection of the extraction function. A real-time surveillance system exploiting monocular camera information was developed to detect, track and monitor the activities of multiple objects [8]. Human parts (head, hands, feet, torso and so on) were located to address the occlusion problem.

* djlee@ee.byu.edu; phone 1 801 422-5923; fax 1 801 422-0201

D.J. Lee, P. Zhan, A. Thomas, R. Schoenberger, "Shape-based Human Intrusion Detection", SPIE International Symposium on Defense and Security, Visual Information Processing XIII, vol. 5438, p. 81-91, Orlando, Florida, USA, April 12-16, 2004.

Other remote monitoring systems can be found in literatures. An intrusion detection system making decision relying on the consensus decision from multiple camera units via a local area network was developed [9]. Two phases of the system were included in the system, hypothesis generation to extract possible threats and hypothesis verification to confirm them. Gabor filtering was used in the second phase. Multiple cameras were involved, which increases the system cost and more processing work need to be done. Another remote monitoring system working in unattended environment was presented [10]. Statistical morphological operator was applied to classify the object, meanwhile achieving the character of being invariant to translation, rotation and scale variations due to the nice properties of the operator. However, a large database is required to guarantee better classification.

Optical flow is the foundation of many human intrusion detection systems. An optical flow-based intrusion detection system was described [11-12]. The biggest concern of the system is to deal with changing background, and complex scenes. Multiple DSP boards were used to implement a real-time system. Detection was done by calculating and extracting the uniform optical flow. But the assumption that intruder has to move at a constant speed has to be made in order for the system to work well. Another research also exploits the information of optical flow [13]. Statistical model was used to help estimate the optical flow. But optical flow is robust enough especially complex conditions. A different approach by applying Radial Reaching Correlation (RRC) between the reference and current scenes to evaluate local textures has been proposed [14].

A system which relies on the Markov random field to solve occlusion problem was mentioned [15]. A system was developed to resort depth information from binocular sequences, which has the similar idea as in [11-12], but no assumption about the way how intruders are moving was made. Other systems using depth information to do the detection work was shown in [17], but different from [16], only monocular camera was used. The advantage is that the system doesn't require the background frame, therefore it works for mobile platform, but however it works well only for the indoor environment, and only deals with simple behavior recognition. Another indoor monitoring system was addressed in [18]. In this system, a prior knowledge about the layout of the room has to be assumed. In [19], Fourier descriptor and a feed-forward neural network are combined together to do the classification work. Two models for the detection system are discussed in [20], and user behavior and statistics, which were called information profiles, were updated to train the system to detect new intrusions. But system resources are a big issue with this kind of algorithm. Another statistical method for detecting humans in images was proposed in [21]. It's one of the appearance-based algorithms, but different from focus on the pixel values directly, it does the recognition based on geometrical structures. Similar to [17], no static background was required for this method; therefore it's good for dynamic scenes. But the algorithm doesn't work when the target and background have the same pixel value on average.

Other human detection techniques dealing with image and video sequences are found in [22-25]. In [22], human silhouette extraction based on image registration technique was discussed. But to utilize the correspondence information, computational complexity was introduced to the system. In [23], a hierarchical method for human detection was presented. A method to extract the whole silhouette of a standing or walking person in still images is discussed in [24]. It has the advantage of being invariant to the changes in intensity, color and texture. In [25], based on Kullback's cross-entropy, a regularization method was proposed to solve the ill-posed estimation problem. But for [23-25], due to the computation requirements, they are more suitable for off-line processing.

In this paper, we present a fast and accurate shape comparison method that compares the contour of a potential threat with the shapes stored in database. This algorithm uses a single camera in an open or remote environment. It does not attempt to solve the occlusion problem or to detect human from a cluttered scene. It does not attempt to analyze human motion or localize human in a video. The input to the system is an image sequence captured from an open environment. We focus on developing an efficient method for representing the contour extracted from the intruder and a fast and accurate method to make real-time early threat assessment. In Section 2, we discussed a simple set up for extracting the contour from the intruder. We present a modified curve evolution method for shape representation in Section 3. In Section 4, we discuss and compared a few shape matching methods and introduce a fast and accurate algorithm to effectively measure shape similarity for matching or recognition. The results of this new method and two other selected methods are included in Section 5. We review this work and draw our conclusion in Section 6.

D.J. Lee, P. Zhan, A. Thomas, R. Schoenberger, "Shape-based Human Intrusion Detection", SPIE International Symposium on Defense and Security, Visual Information Processing XIII, vol. 5438, p. 81-91, Orlando, Florida, USA, April 12-16, 2004.

2. SHAPE EXTRACTION

We used a differential motion analysis (DMA) method to detect the scene change in the area. The difference between the reference and test images was used to extract the object contour [26-27]. This DMA method is very effective because the illumination variations can be eliminated through subtraction. Polygon approximation using a new curve evolution method was then applied to the extracted contour to remove the edge noise and eliminate redundant data points so that all objects can be represented with a fixed number of points [28-30]. Shape representation techniques such as turn angle and bend angle function were used to describe shapes in a way that they will be invariant to translation, rotation, and scaling [26, 31-32]. Finally, shape features can be used to measure similarity between the test contour and the contours stored in the database.

The intrusion detection system stores the shape features of possible objects through training. These shape features are obtained from images taken from different angles, distances, and locations. Shape features of the test objects were calculated from the contour and compared against the shape features in the database. Shape features that show the highest similarity measure or the lowest dissimilarity measure represent the best match. In other words, the intrusion can be identified by finding the best shape match in the database. The processing diagram in Fig. 1 shows the data flow and illustrates the processing steps.

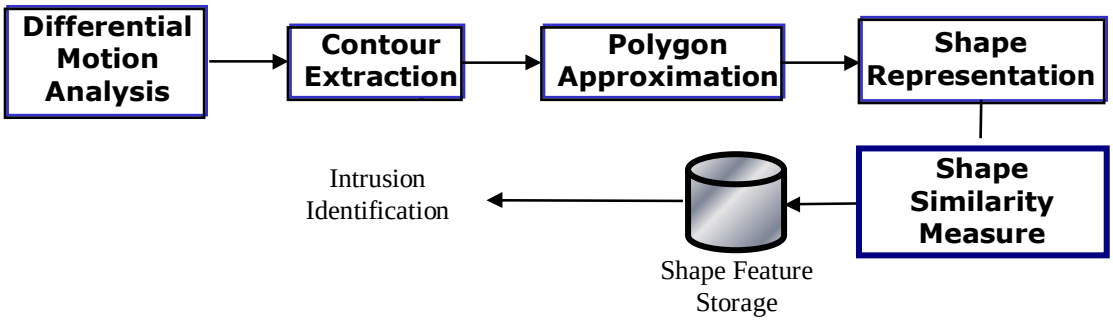

Figure 1. Processing Diagram.

DMA can be done in two ways. One is to find the difference between the input image and the stored reference background. The other one is to calculate the difference between two consecutive frames. The first one can provide better contour extraction result but requires reference background images for different illumination conditions. The algorithms must either have the capability of auto-calibration or auto-selection of the reference image from image database. The later approach minimizes the effect of illumination variations but does not provide very clear contour for process. Figs. 2 and 3 illustrate both methods and the anticipated results.

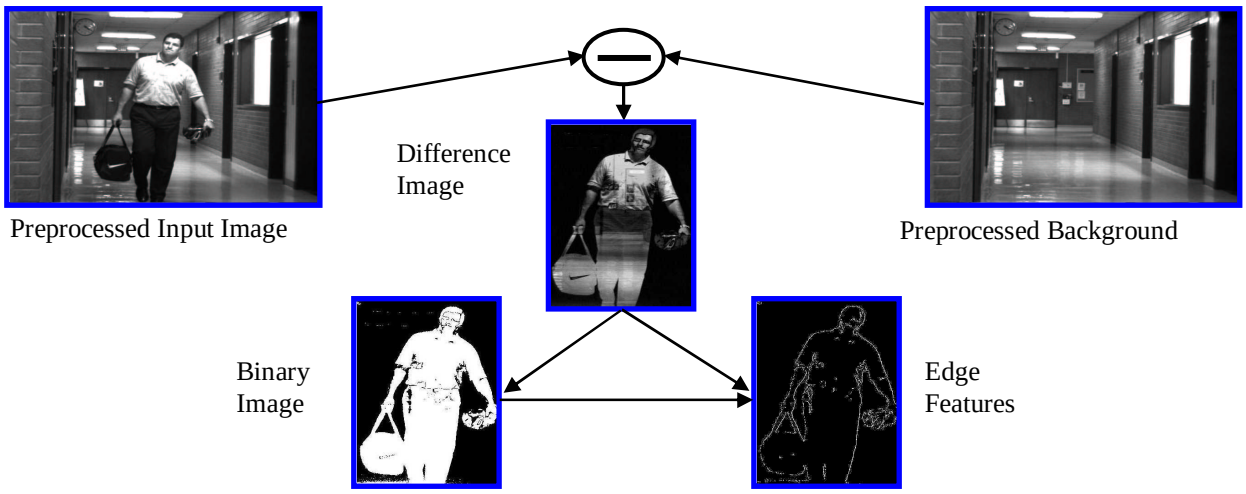

Figure 2. Differential motion analysis using a reference background.

D.J. Lee, P. Zhan, A. Thomas, R. Schoenberger, "Shape-based Human Intrusion Detection", SPIE International Symposium on Defense and Security, Visual Information Processing XIII, vol. 5438, p. 81-91, Orlando, Florida, USA, April 12-16, 2004.

In Fig. 2, the selected reference image was subtracted from the input image to provide the difference image. A linear threshold can be selected to binarize the difference image. Object contours can then be extracted using edge operator such as Sobel or Canny edge operator. In Fig. 3, two consecutive frames from the input video signal are used to determine the change on the scene. Similarly, edge operators can be used to detect the object boundary. We implemented and tested both methods using real-life images. In this paper, all contours were extracted using the first method in order to provide better contours for developing shape matching algorithms.

Figure 3. Differential motion analysis using two consecutive frames

3. SHAPE REPRESENTATION

Shape descriptors and classification algorithms must be invariant to translation, rotation, and scaling because objects can be viewed from different angles, locations, and with varying size. In order to accurately classify intrusion objects, it is first necessary to reduce the number of data points on the contour to a reasonable number that can be evaluated using shape similarity measurement. Many of the data points obtained in the contour extraction algorithm are redundant. Additionally, we want to filter out the data points that contain edge noise. We found that a reduced data set of 60 points was sufficient to retain the important shape features for comparison. Another reason for reducing data points is to be able to represent contours in tangent space for l_2 norm calculation or using bend angle function for calculating Fourier descriptors.

3.1 Data Point Reduction

Data reduction can be accomplished through a curve evolution technique that iteratively compares all the relevance measures of the vertices on the contour [28-30]. A higher relevance measure means that the vertex makes a larger contribution to the overall shape of the contour, and thus is more important to be retained. For each iteration, the vertex with the lowest relevance was removed and a new polygon was created by connecting the remaining vertices with a straight line. We modified the relevance measure, K, for the curve evolution method in [28-30] to remove redundant points while maintaining the significance of the contours. The new relevance measure is shown in (1) where β is the turn angle on the vertex between line segments s_1 and s_2 and $l(s_1)$ and $l(s_2)$ are the normalized length from the vertex to the two adjacent vertices [33-35].

$$K(s_1,s_2)=\frac{|(\beta(s_1,s_2)-180)|\,l(s_1)l(s_2)}{l(s_1)+l(s_2)} \qquad (1)$$

This modified curve evolution method reduces short, straight line segments that provide little information about the overall shape of the object. This method preserves a fixed number of data points (60) for each contour, which makes it easier to measure shape similarity. Unlike equal space sampling that may lose data points containing significant shape information, this modified curve evolution preserves detail shape information. Fig. 4 (a) shows the original data set of a dog that was obtained from the contour extraction algorithm. Fig. 4 (b) shows the reduced data set obtained using Equation (1). Although there is a slight distortion in the shape of Fig. 4 (b), the basic shape and the detail of the object was retained. These 60 data points, although not equally spaced, make the most significant contribution to the shape and can be easily used for shape representation. Fig. 4 (c) shows the 60 data points obtained by equal space sampling. It contains redundant data points which should be removed because they form a straight line. It also loses the detail of the contour especially on the round corners or curves. Fig. 5 shows two more examples of the data reduction result, one for a human contour and the other one for a vehicle.

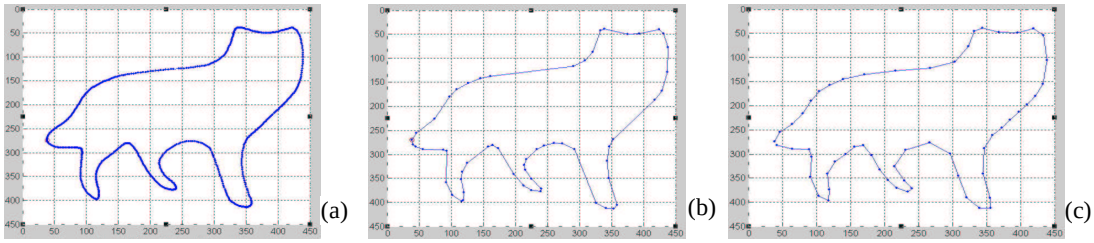

(a) (b) (c)

Figure 4. (a) Original data set, (b) reduced to 60 points using Equation 1, and (c) equal space sampling.

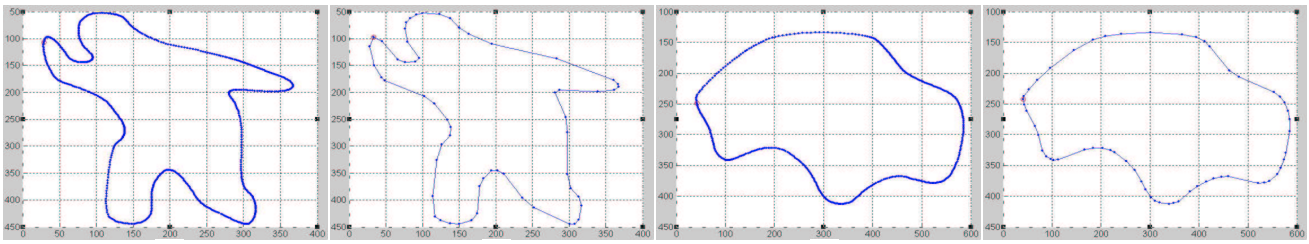

(a) (b) (c) (d)

Figure 5. (a) Original data set of a human, (b) its 60-point representation,
(c) the original data set of a vehicle, and (d) its 60-point representation.

3.2 Tangent Space and Bend Angle

Polygon approximation of the reduced data points can be expressed as turn angle vs. normalized length (tangent space) or bend angle vs. normalized length. The turn angle is calculated for each segment by referencing to the horizontal line. The bend angle is calculated so that the clockwise turn gives a negative angle whereas a counter clockwise turn gives a positive angle. The representations of these two functions are shown in Fig. 6.

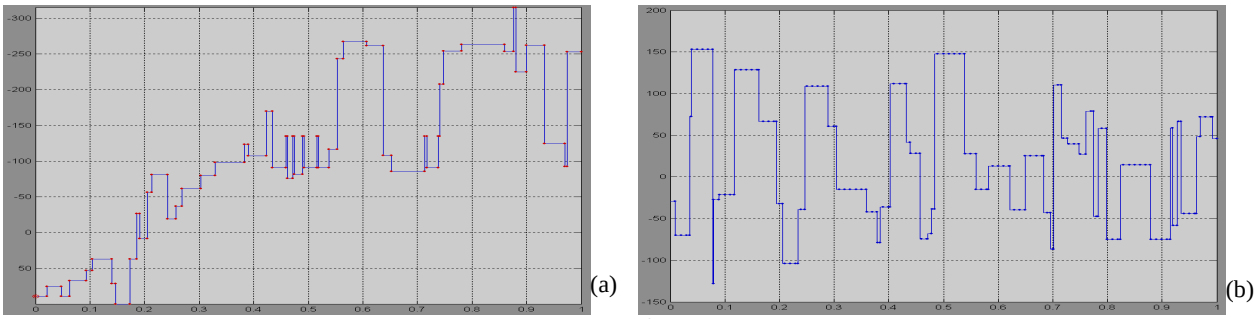

(a) (b)

Figure 6. (a) Turn angle and (b) bend angle function vs. normalized length

They are both represented as a function of normalized length to meet the scaling invariant requirement. They are translation invariant because the turn angle or bend angle and length do not contain information about the shape location. The object rotation angle becomes irrelevant when calculating the turn angle and bend angle functions because they are both based on the relative angles. In other words, both functions will stay the same even if the object is rotated, translated, or resized. Depending on the data point selected as the first point in the data sequence, these two functions may shift along the x axis. Moreover, rotation will cause the turn angle function to shift along the y axis.

4. SHAPE MATCHING

We reviewed different shape matching methods that are capable of reporting similarity between shapes. Methods reviewed include global shape characteristics such as perimeter, convex perimeter, major axis length and angle, minor axis length and angle, compactness, and roughness, invariant moments, polygon approximation, and Fourier descriptors. From our past research work [36-38], we learned that the first two methods do not yield accurate matching results especially for minor shape variations. In this paper we used turn angle function to represent shapes in tangent

space and computed shape similarity using l_2-*norm.* Alignment of two turn functions for similarity measurement is a time consuming process. We developed a much faster matching algorithm that uses power cepstrum to align two similar signals before the similarity can be measured. We also used bend angle function for shape representation and computed Fourier descriptors for performance evaluation.

4.1 Tangent Space Searching

An important requirement for shape similarity measure is that the shift on the starting point of the polygon should not have any effect on similarity measurement calculations. For rotation or starting point shift, turn function remains the same except shifting vertically when there is a rotation and moving horizontally when there is a shift in starting point. This means turn functions of two shapes must be aligned to compensate for the shifts caused by rotation and starting point shift before they can be compared. The distance between two turn functions, Θ_A and Θ_B , can be measured as

$$\delta_2(A,B) = \|\Theta_A - \Theta_B\|_2 = \sqrt{(\int_0^1 |\Theta_A - \Theta_B|^2 ds)} = \sqrt{\min_{\theta\in R, t\in[0,1]} (\int_0^1 |\Theta_A(s+t) - \Theta_B(s) + \theta|^2 ds)} \quad (2)$$

In most cases, the two turn functions are not identical because of the differences in shape. The alignment can only be achieved through minimizing the distance while shifting one turn function. In other words, the distance between two turn functions is obtained by performing a two-dimensional search to find the minimum distance. Another approach is to reduce the search to one dimension by calculating the best value of the turn angle θ [28-30]. The best value of θ is a function of length shift *t* in the x axis to minimize

$$h(t,\theta) = \int_0^1 |\Theta_A(s+t) - \Theta_B(s) + \theta|^2 ds \quad \text{when} \quad (3)$$

$$\theta'(t) = \int_0^1 (\Theta_B(s) - \Theta_A(s+t))\, ds = \alpha - 2\pi t \quad \text{,where } \alpha = \int_0^1 \Theta_B(s)\, ds - \int_0^1 \Theta_A(s)\, ds \,. \quad (4)$$

For each searching step in x (length) direction, the best value of θ was calculated according to Equation 4. The distance δ was calculated and recorded. After shifting the turn function through the searching range, the minimum δ is the distance between the two turn functions. Fig. 7 shows the one dimensional searching result for comparing two shapes expressed as turn functions. The difference between the two shapes (dissimilarity) can be calculated as the total distance between two aligned signals.

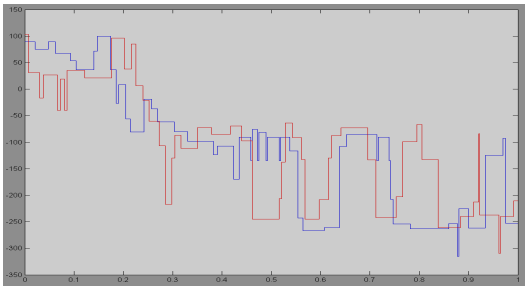

Figure 7. Two aligned normalized turn angle functions in tangent space.

4.2 Matching Bend Angle Functions Using Fourier Descriptors

For the bend angle function approach, the Fourier descriptors can be used to measure the similarity between two shapes. The Fourier expansion of Θ(*l*) is expressed as

$$\Theta(l) = \mu_0 + \sum_{n=1}^{\infty} (a_n \cos nl + b_n \sin nl) \quad (5)$$

, where a_n and b_n are coefficients for each frequency component. Since Θ(*l*) is a step function, μ_0, a_n, *and* b_n *can be derived as*

$$\mu_0 = -\pi - \frac{1}{L}\sum_{k=1}^{m} \lambda_k \theta_k$$

$$a_n = -\frac{1}{n\pi}\sum_{k=1}^{m} \theta_k \sin\frac{2\pi n \lambda_k}{L} \qquad b_n = \frac{1}{n\pi}\sum_{k=1}^{m} \theta_k \cos\frac{2\pi n \lambda_k}{L} \quad (6)$$

$$\textit{where } \lambda_k = \sum_{i=1}^{k} l_i \quad \textit{and} \quad L = \sum_{i=1}^{m} l_i = \textit{the total length}$$

D.J. Lee, P. Zhan, A. Thomas, R. Schoenberger, "Shape-based Human Intrusion Detection", SPIE International Symposium on Defense and Security, Visual Information Processing XIII, vol. 5438, p. 81-91, Orlando, Florida, USA, April 12-16, 2004.

Power spectrum of the bend angle function is invariant to the shift in length (l in this case). Because of this property, Fourier descriptors of a bend angle function (function of normalized length) meet all invariant requirements for shape description for shape matching using the bend angle function. Power spectrum (A_n) and phase angle information (F_{jk}) can be calculated as follow [31,32] :

$$A_n = \sqrt{a_n^2 + b_n^2} \quad and \quad \alpha_n = \tan^{-1}(b_n / a_n)$$
$$F_{jk} = j^* \alpha_k - k^* \alpha_j \quad where \; j^* = j / \gcd(j,k) \tag{7}$$
$$\gcd : greatest\ common\ divisor$$

Fig. 8 shows the Fourier descriptors of the bend angle function shown in Fig. 6 (b). Similarity measure can then be derived based on the difference between two sets of Fourier descriptors.

4.3 Matching Turn Functions Using Power Cepstrum

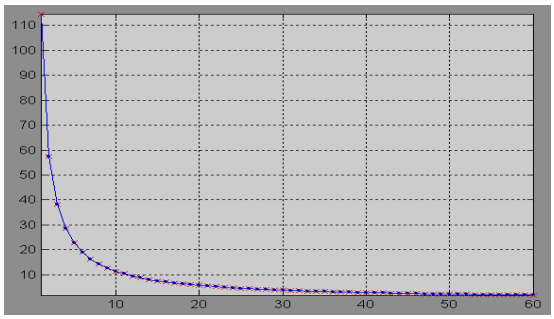

Figure 8. Fourier descriptors of a normalized bend angle function.

As shown in Section 4.1, matching in tangent space can be simplified to a 1D search. The best estimated value θ can be calculated in Equations 4. However, searching in turn angle is still a time consuming process. In this section we introduced a new searching method that uses power cepstrum technique. The cepstrum technique was first described by Bogert et al. in 1962 [38-42]. It was used to analyze data containing echoes. This technique can be divided into power cepstrum and complex cepstrum. Power cepstrum is usually used to determine the echoes while complex cepstrum can be used to both detect and remove the echoes. This technique has been extended to analyze 2D signals for image registration and 3D vision [43-46]. We chose cepstrum technique over phase correlation method because of better noise tolerance [44, 47], which is equivalent to the shape difference that can be seen in matching two turn functions.

Power Cepstrum is defined as the power spectrum of the logarithm of the power spectrum of a signal [40-42]. This definition can be expressed in Equation 8 as:

$$power\ cepstrum = \left| F(\ln(\left| F(\Theta(l)) \right|^2)) \right|^2 \tag{8}$$

, where $\Theta(l)$ is the turn function and $|F(.)|^2$ is the power spectrum. In our turn angle function matching application, $\Theta(l)$ is the superposition of two turn angle functions, $\Theta_A(l)$ and $\Theta_B(l)$ as shown in Section 4.1. In ideal cases, the only differences between these two turn angle functions are a scale factor α that represents the rotation between two shapes and an index shift l_o between two functions. This is shown in Equation 9 as:

$$\Theta(l) = \Theta_A(l) + \Theta_B(l) = \Theta_A(l) + \alpha\, \Theta_A(l - l_o) \tag{9}$$

The result of applying power cepstrum to $\Theta(l)$ is

$$P[\Theta(l)] = \left| F(\ln(\left| F(\Theta_A(l)) \right|^2)) \right|^2 + A\delta(l) + B\delta(l \pm l_o) + C\delta(l \pm 2l_o) + \cdots$$
$$= \text{power cepstrum of the reference turn function } \Theta_A \text{ plus a train of impulses}$$
$$\text{occurring at integer multiples of the shift } l_o \tag{10}$$

By detecting the occurrence of these impulses, shape indexing shift can be determined. The distance (dissimilarity) between the two turn angle functions can be calculated by aligning the two functions according to the detected shape indexing shift.

In turn angle function matching application, the ideal case shown in Equation 9 will not be possible because there will be difference between two contours. Power cepstrum result will have noise around the impulses that makes the detection of the local maxima difficult. However, inaccurate detection of the impulses will yield incorrect shape indexing shift which will increase the dissimilarity value. This results in higher dissimilarity for shapes that are different and lower dissimilarity for shapes that are similar. Impulses can be detected accurately when comparing similar shapes as shown in Fig. 9. In Fig. 9(b) two very similar contours with different data point indexing show a small shift between turn functions. Impulses can be detected accurately as shown in Fig. 9(c). However, when there are noticeable differences between two contours, power cepstrum result will be affected and the detection of impulses will not be as accurate. Figure 10 (a) shows turn functions of two identical contours but with rotation, scaling, and shift in data indexing. Power cepstrum result is not affected by these variations as shown in Fig. 10(b). Fig. 10 (c) shows turn functions of two contours with noticeable differences. Power cepstrum result becomes noisy and although impulses may not be a good indication of the index shift, the shape similarity measurement still shows that they are different.

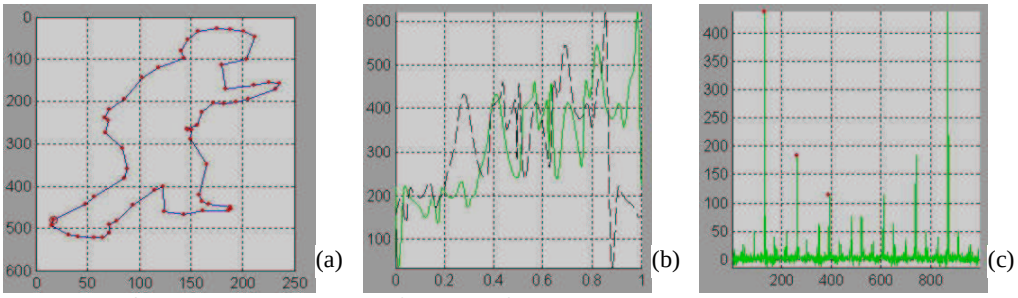

Figure 9. (a) Contour after data reduction, (b) turn functions of two very similar contours, and (c) power cepstrum result.

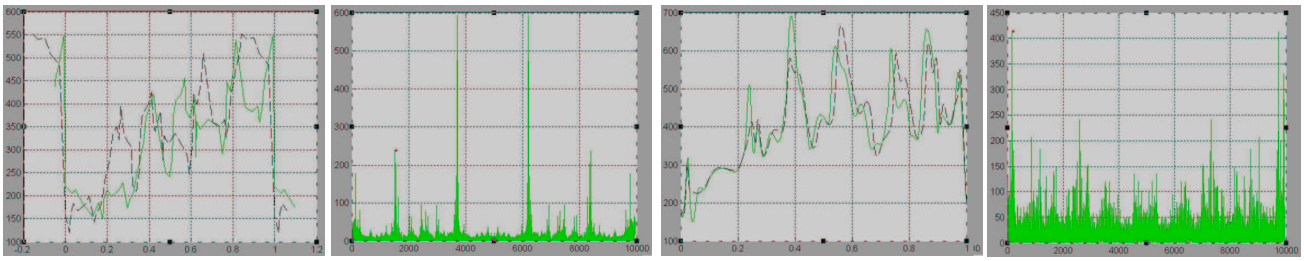

Figure 10. (a) Turn functions of two identical contours but with different data point indexing, scaling, and rotation. (b) Power cepstrum result. (c) Turn functions of two contours with noticeable difference. (d) Power cepstrum result of (c).

5. TEST RESULTS

We collected total 156 images for the experiment. This data set includes 57 images from different animals, 54 images from human with different poses, and 45 from different types of vehicles. Fig. 11 shows a few examples of the extracted contours.

All three matching methods discussed in Section 4 were implemented and tested with this data set. Each contour was used to compare against other contours in the data set. Matching result (dissimilarity) was recorded and ranked to determine the best matched shape category. Performance was evaluated using precision and recall method. Table 1 shows the summary of test result. Matching in tangent space has the highest human intrusion detection precision of 96.3% (52/54) and the lowest recall of 7.8% (8/102). Using Fourier descriptors for matching bend angle function has the lowest precision of only 37% (20/54) and the highest recall of 30.4% (31/102). Power cepstrum matching has slightly lower precision of 92.6% and slightly higher recall of 9.8% than the tangent space matching. However, the performance difference between the two methods is insignificant comparing with the processing speed improvement that the cepstrum technique can provide.

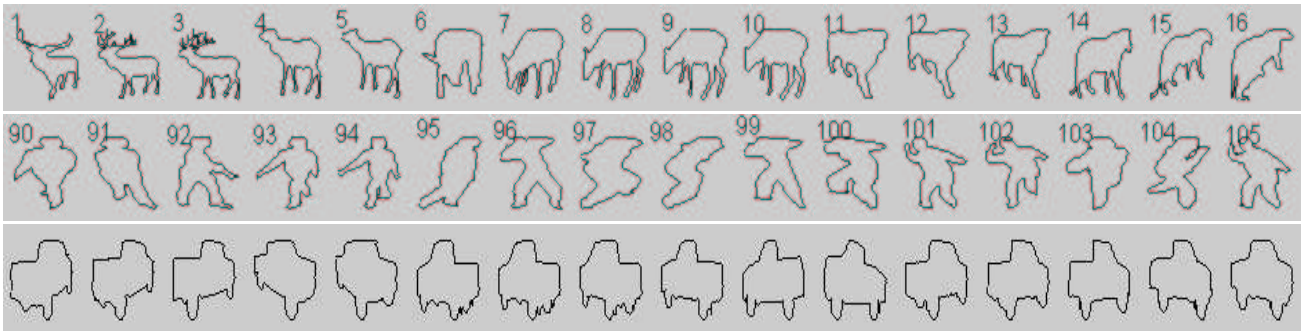

Figure 11. Examples of extracted contours including animal, human, and vehicle.

Table 1. Intrusion Detection Results

Category	Number Used	Classified as Human	Classified as Animal	Classified as Vehicle
Human	54	52	2	0
Animal	57	8	40	9
Vehicle	45	0	0	45

Tangent Space Searching

Category	Number Used	Classified as Human	Classified as Animal	Classified as Vehicle
Human	54	20	16	18
Animal	57	16	34	7
Vehicle	45	15	8	45

Fourier Descriptors of Bend Angle Function

Category	Number Used	Classified as Human	Classified as Animal	Classified as Vehicle
Human	54	50	3	1
Animal	57	10	37	10
Vehicle	45	0	0	45

Power Cepstrum Matching

6. CONCLUSIONS

We measured shape similarity between two contours to determine if the intrusion is indeed a human or some other objects. We selected three categories, human, animal, and vehicle, for comparisons. We developed a matching technique using power cepstrum to align two turn angle functions for comparison for human intrusion detection. We implemented two other methods to compare the performance. Although the performance of power cepstrum is slightly lower than the tangent space search, it improves the searching process greatly. More testing will be conducted to verify our results.

REFERENCES

1. Wang, Liang, Hu, Weiming, *Recent development in human motion analysis*, Pattern Recognition, vol. 36(3), pp 585-601, Mar., 2003
2. Aggarwal, J.K., Cai, Q., *Human motion analysis: A Review*, Computer Vision and Image Understanding, vol.73 (3), pp 428-440, Mar., 1999
3. Wong, Kwok-Wai, Lam, Kin-Man, *A robust scheme for live detection of human faces in color images*, Signal Processing: Image Communication, vol. 18 (2), pp 103-114, Feb., 2003
4. Kouzani, A. Z., *Locating human faces within images*, Computer Vision and Image Understanding, vol. 91 (3), pp 247-279, Sept., 2003
5. Pham, Thang V., Worring, Marcel, *Face detection by aggregated Bayesian network classifiers*, Pattern Recognition Letters, vol. 23 (4), pp 451-461, Feb., 2002

D.J. Lee, P. Zhan, A. Thomas, R. Schoenberger, "Shape-based Human Intrusion Detection", SPIE International Symposium on Defense and Security, Visual Information Processing XIII, vol. 5438, p. 81-91, Orlando, Florida, USA, April 12-16, 2004.

6. Henry, T., Ruwan Janapriya, E., *An automatic system for multiple human tracking and actions recognition in office environment*, Proceedings of 2003 IEEE International Conference on Acoustics, Speech, and Signal Processing (ICASSP '03), vol.3, pp III - 45-8, Apr., 2003
7. Kuno, Y., Watanabe, T., *Automated detection of human for visual surveillance system*, Proceedings of the 13th International Conference on Pattern Recognition, vol.3, pp 865-869, Vienna, Austria, Aug., 1996
8. Haritaoglu, I., Harwood, D., *W4: real-time surveillance of people and their activities*, IEEE Transactions on Pattern Analysis and Machine Intelligence, vol. 22(8), pp 809-830, Aug., 2000
9. Yuan, Xiaojing, Sun Zehang, *A distributed visual surveillance system*, Proceedings of IEEE Conference on Advanced Video and Signal Based Surveillance, pp 199-204, Jul., 2003.
10. Foresti, G.L., *A real-time system for video surveillance of unattended outdoor environments*□ IEEE Transactions on Circuits and Systems for Video Technology, vol. 8(6), pp 697-704, Oct., 1998
11. Iketani, A., Nagai, A., *Detecting persons on changing background*, Proceedings of Fourteenth International Conference on Pattern Recognition, vol.1, pp 74-76, Brisbane, Australia, Aug., 1998.
12. Iketani, A., Kuno, Y., *Real-time surveillance system detecting persons in complex scenes*, Proceedings of International Conference on Image Analysis and Processing, pp 1112-1115, Venice Italy, Sept., 1999
13. Fablet, R., Black, M.J., Automatic *Detection and Tracking of Human Motion with a View-Based Representation*, Computer Vision - ECCV 2002, Proceedings of 7th European Conference on Computer Vision, Part I, vol. 2350, p.476, Copenhagen, Denmark, May, 2002.
14. Satoh, Y., Tanahashi, H., *Robust human detection from complex background by radial reach filter*, TENCON '02. Proceedings of 2002 IEEE Region 10 Conference on Computers, Communications, Control and Power Engineering, vol. 1, pp 533 – 536, Oct., 2002
15. Eng, w-Lung, Kam, A.H., Human *detection and tracking within hostile aquatic environments*, Proceedings of 12th International Conference on Image Analysis and Processing, pp 133-138, Sept., 2003.
16. Ran, Yang, Qinfen Zheng, *Multi moving people detection from binocular sequences*, Proceedings of IEEE International Conference on Acoustics, Speech, and Signal Processing, (ICASSP '03), vol.3, pp III - 37-40, Apr., 2003.
17. Xu, Fengliang, Kikuo Fujimura, *Human detection using depth and gray images*, Proceedings of IEEE Conference on Advanced Video and Signal Based Surveillance, pp 115-121, Jul., 2003.
18. Ayers, Douglas, Shah, Mubarak, *Monitoring human behavior from video taken in an office environment*, Image and Vision Computing, vol. 19 (20), Oct., 2001
19. Toth, D., Aach, T., *Detection and recognition of moving objects using statistical motion detection and Fourier descriptors*, Proceedings of 12th International Conference on Image Analysis and Processing, pp 430 – 435, Sept., 2003.
20. Okazaki, Y., Sato, I, *A new intrusion detection method based on process profiling*, Proceedings of 2002 Symposium on Applications and the Internet, pp 82 – 90, Nara, Japan, Feb., 2002
21. Utsumi, A., Tetsutani, N., *Human detection using geometrical pixel value structures*, Proceedings of Fifth IEEE International Conference on Automatic Face and Gesture Recognition, pp 34-39, Washington DC, USA, 2002.
22. Ju Han, Bhanu, B., *Detecting moving humans using color and infrared video*, Proceedings of IEEE International Conference on Multisensor Fusion and Integration for Intelligent Systems, MFI2003, pp 228-233, Aug., 2003
23. Ozer, B., Wolf, W., *Human activity detection in MPEG sequences*, Proceedings of Workshop on Human Motion, pp 61-66, Los Alamitos, CA USA, Dec., 2000.
24. Ozer, B., Wolf, W., *Human detection in compressed domain*, Proceedings of 2001 International Conference on Image Processing, vol.3, pp 274-277, Thessaloniki, Greece, Oct., 2001
25. Wang, Yaming, Baciu George, *Human motion estimation from monocular image sequence based on cross-entropy regularization*, Pattern Recognition Letters, vol. 24(1-3), pp 315-325, Jan., 2003
26. Shapiro, L. and Stockman, G., *Computer Vision*, Prentice-Hall Inc., Upper Saddle River, New Jersey , 2001.
27. Sonka, M., Hlavac, V., and Boyle, R., *Image Processing, Analysis, and Machine Vision*, PWS Publishing, 1999.
28. Latecki, L.J. and R. Lakämper, "Application Of Planar Shape Comparison To Object Retrieval In Image Databases". Pattern Recognition, 35(1):15-29, 2002.
29. Latecki, L.J. and R. Lakämper, " Shape Description and Search for Similar Objects in Image Databases", *State-of-the-Art in Content-Based Image and Video Retrieval*, Kluwer Academic Publishers, 20001.
30. Arkin, Esther M., L. Paul Chew, Daniel P. Huttenlocher, Klara Kedem, and Joseph S. B. Mitchell, "An Efficient Computable Metric for Comparing Polygon Shapes", IEEE Transactions on Pattern Analysis and Machine Intelligence, vol. 13, no. 3, pp. 209-216, March 1991.

D.J. Lee, P. Zhan, A. Thomas, R. Schoenberger, "Shape-based Human Intrusion Detection", SPIE International Symposium on Defense and Security, Visual Information Processing XIII, vol. 5438, p. 81-91, Orlando, Florida, USA, April 12-16, 2004.

31. Gonzalez, Rafael and Richard Woods, *Digital Image Processing*, pp.655-659, Prentice Hall, 2002
32. Zahn, Charles and Ralph Roskie, "Fourier Descriptors for Plane Closed Curves", *IEEE Transaction on Computer*, vol. C-21, no. 3, March 1972.
33. D. J. Lee, Sharon Redd, Robert Schoenberger, Xiaoqian Xu, and Pengcheng Zhan, "An Automated Fish Species Classification and Migration Monitoring System", *Proceedings of The 29th Annual Conference of the IEEE Industrial Electronics Society*, Roanoke, Virginia, November 2-6, 2003.
34. D. J. Lee, Daniel Bates, Christopher Dromey, and Xiaoqian Xu, "A Vision System Performing Lip Shape Analysis for Speech Pathology Research", *Proceedings of The 29th Annual Conference of the IEEE Industrial Electronics Society*, Roanoke, Virginia, November 2-6, 2003.
35. D.J. Lee, D.M. Bates, C. Dromey, X. Xu, and S. Antani, "An Imaging System Correlating Lip Shapes and Tongue Contact Patterns for Speech Pathology Research", *Proceedings of The 16th IEEE Symposium on Computer-Based Medical Systems*, p. 307-313, New York, NY, USA, June 26-27, 2003.
36. D.J. Lee, S. Antani, and L.R. Long, *"Similarity Measurement Using Polygon Curve Representation and Fourier Descriptors for Shape-based Vertebral Image Retrieval"* SPIE Medical Imaging, Image Processing, vol. 5032, p. 1283-1291, San Diego, CA, USA, February 16-20, 2003.
37. L.R. Long, S. Antani, D.J. Lee, D. Krainak, and G.R. Thoma, *"Biomedical Information from a National Collection of Spine X-rays: Film to Content-based Retrieval"*, SPIE Medical Imaging, PACS and Integrated Medical Information Systems: Design and Evaluation, vol. 5033, p. 70-84, San Diego, CA, USA, February 16-20, 2003.
38. S. Antani, L.R. Long, G.R. Thoma, and D.J. Lee, "*Evaluation of Shape Indexing Methods for Content-Based Retrieval of X-Ray Images*", SPIE Electronic Imaging, Storage and Retrieval for Media Databases, vol. 5021, p. 405-416, Santa Clara, CA, USA, January 19-23, 2003.
39. B. P. Bogert, M. J. R. Healy, and J. W. Tukey, "The Quefrency Analysis of Time Series of Echoes: Cepstrum and Saphe Cracking," in Proceedings, Symposium held at Brown U., 11-14 July 1962, p. 209, M. Rosenblatt, Ed. (Wiley, New York, 1963).
40. D. E. Dudgeon, "The Computation of Two-Diemnsional Cepatra," IEEE Trans. Acoustic Speech Signal processing, ASSP-25, 476 (1977).
41. D. G. Childers, D. P. Skinner, and R.C. Kemerait, "The Cepstrum: A Guide to Processing,", Proceedings, IEEE 65, 1428 (1977).
42. R.C. Kemerait and D. G. Childers, "Signal Detection and Extraction by Cepstrum Techniques," IEEE Trans. Inf. Theory IT-18, 745 (1972).
43. D.J. Lee, S. Mitra, and T.F. Krile, *"Analysis of Sequential Complex Images Using Feature Extraction and 2-D Cepstrum Techniques"*, Journal of Optical Society of America, vol. 6, p. 863-870, June 1989.
44. D.J. Lee, T.F. Krile, and S. Mitra, *"Power Spectrum and Cepstrum Techniques Applied to Image Registration"*, Applied Optics, vol. 27, p. 1099-1106, March, 1988.
45. S. Mitra, D.J. Lee, and T.F. Krile, *"3-D Representation from Time-Sequenced Biomedical Images Using 2-D Cepstrum"*, IEEE Intl. Conference on Visualization in Biomedical Computing, p. 401-408, Atlanta, GA, May 1990.
46. D.J. Lee, S. Mitra, and T.F. Krile, *"Accuracy of Depth Information from Cepstrum-Disparities of a Sequence of 2-D Projections"*, SPIE in Intelligent Robots and Computer Vision, vol. 1192, p. 778-788, Philadelphia, PA, November 1989.
47. D.J. Lee, S. Mitra, and T.F. Krile, *"Noise Tolerance of Power Cepstra and Phase Correlation in Image Registration"*, Optical Society of America Meeting, Santa Clara, CA, November 1988.